

UNIVERSITY OF BIRMINGHAM

University of Birmingham
Research at Birmingham

Use of a stress-minimisation paradigm in high cell density fed-batch *Escherichia coli* fermentations to optimise recombinant protein production.

Wyre, Christopher; Overton, Timothy

DOI:

[10.1007/s10295-014-1489-1](https://doi.org/10.1007/s10295-014-1489-1)

License:

None: All rights reserved

Document Version

Peer reviewed version

Citation for published version (Harvard):

Wyre, C & Overton, T 2014, 'Use of a stress-minimisation paradigm in high cell density fed-batch *Escherichia coli* fermentations to optimise recombinant protein production.', *Journal of Industrial Microbiology and Biotechnology*, vol. 41, no. 9, pp. 1391-1404. <https://doi.org/10.1007/s10295-014-1489-1>

[Link to publication on Research at Birmingham portal](#)

Publisher Rights Statement:

The final publication is available at Springer via: <http://dx.doi.org/10.1007/s10295-014-1489-1>.

Eligibility for repository checked January 2015

General rights

Unless a licence is specified above, all rights (including copyright and moral rights) in this document are retained by the authors and/or the copyright holders. The express permission of the copyright holder must be obtained for any use of this material other than for purposes permitted by law.

- Users may freely distribute the URL that is used to identify this publication.
- Users may download and/or print one copy of the publication from the University of Birmingham research portal for the purpose of private study or non-commercial research.
- User may use extracts from the document in line with the concept of 'fair dealing' under the Copyright, Designs and Patents Act 1988 (?)
- Users may not further distribute the material nor use it for the purposes of commercial gain.

Where a licence is displayed above, please note the terms and conditions of the licence govern your use of this document.

When citing, please reference the published version.

Take down policy

While the University of Birmingham exercises care and attention in making items available there are rare occasions when an item has been uploaded in error or has been deemed to be commercially or otherwise sensitive.

If you believe that this is the case for this document, please contact UBIRA@lists.bham.ac.uk providing details and we will remove access to the work immediately and investigate.

1 **Use of a stress-minimisation paradigm in high cell density fed-batch *Escherichia coli* fermentations**
2 **to optimise recombinant protein production**

3 Chris Wyre and Tim W Overton*

4 Bioengineering, School of Chemical Engineering, and Institute of Microbiology & Infection, University
5 of Birmingham, Edgbaston, Birmingham B15 2TT, UK

6 *Corresponding author: t.w.overton@bham.ac.uk

7 Telephone: +44 (0) 121 414 5306

8 Fax: +44 (0) 121 414 5324

9 **ABSTRACT**

10 Production of recombinant proteins is an industrially important technique in the biopharmaceutical
11 sector. Many recombinant proteins are problematic to generate in a soluble form in bacteria as they
12 readily form insoluble inclusion bodies. Recombinant protein solubility can be enhanced by
13 minimising stress imposed on bacteria through decreasing growth temperature and the rate of
14 recombinant protein production. In this study, we determined whether these stress minimisation
15 techniques can be successfully applied to industrially-relevant high cell density *Escherichia coli*
16 fermentations generating a recombinant protein prone to forming inclusion bodies, CheY-GFP. Flow
17 cytometry was used as a routine technique to rapidly determine bacterial productivity and
18 physiology at the single cell level, enabling determination of culture heterogeneity. We show that
19 stress-minimisation can be applied to high cell density fermentations (up to a dry cell weight of > 70
20 g·L⁻¹) using semi-defined media and glucose or glycerol as carbon sources, and using early or late
21 induction of recombinant protein production, to produce high yields (up to 6 g·L⁻¹) of aggregation-
22 prone recombinant protein in a soluble form. These results clearly demonstrate that stress
23 minimisation is a viable option for the optimisation of high cell density industrial fermentations for

24 the production of high yields of difficult-to-produce recombinant proteins, and present a workflow
25 for the application of stress minimisation techniques in a variety of fermentation protocols.

26 **Keywords:** Green fluorescent protein; fed-batch fermentation; flow cytometry; inclusion bodies

27

28 INTRODUCTION

29 Production of recombinant proteins in bacterial hosts is an important part of the biopharmaceutical
30 industry. Although many new biopharmaceutical drugs (such as monoclonal antibodies) are made in
31 mammalian hosts, bacterial hosts are undergoing a resurgence in popularity not only for relatively
32 simple protein and peptide drugs (such as insulin) but also for more complex molecules such as
33 antibody fragments. Of the 58 biopharmaceutical drugs approved between 2006 and June 2010, 17
34 were produced in *E. coli* [29]. Efficient production of soluble recombinant proteins is also essential
35 for generation of proteins for structural studies that are the basis of the development of new drug
36 ligand molecules.

37 Two major routes are utilised for recombinant protein production in bacterial hosts. First, the
38 recombinant protein can be generated in the form of inclusion bodies (IBs); dense intracellular
39 particles comprising mainly misfolded protein but also containing some correctly folded, functional
40 protein [6]. Many recombinant proteins have a tendency to form IBs in bacterial hosts for a number
41 of reasons including differences in folding pathways and physicochemical conditions between
42 bacteria and eukaryotic cells [14]. Inclusion bodies are relatively simple to generate to high yields,
43 are easy to purify due to their density, and are a relatively pure source of recombinant protein [21].
44 However, to generate functional protein, IBs must be denatured (usually chemically) and then the
45 protein must be refolded; this refolding step varies in success and yield, such that some recombinant
46 proteins cannot be successfully refolded.

47 Alternatively, the recombinant protein may be synthesised in a correctly-folded, soluble form, and
48 purified in this functional form [22]. This is especially desirable for recombinant proteins with
49 multiple isoforms and for structural determination studies. However, there are many potential
50 problems with this approach, and some recombinant proteins cannot be readily synthesised in
51 bacteria in a soluble form. Often, attempts to produce soluble recombinant protein lead to IB
52 formation, decreases in host cell viability, loss of recombinant protein-encoding plasmids and
53 overgrowth of non-producing, plasmid-free bacteria, all of which can lead to low biomass and
54 recombinant protein yields. Indeed, many recombinant proteins that are difficult to produce are
55 referred to as 'toxic' proteins, due to the apparently toxic effects on host bacteria [17]. Nonetheless,
56 soluble production frequently represents a desirable recombinant protein production route.

57 Previous studies have attempted to increase the proportion of soluble recombinant protein
58 generated in bacterial hosts using a variety of methods. Some recombinant proteins can be induced
59 to fold using modulation of chaperones, a class of proteins that assist protein folding (Reviewed by
60 [10]). This can be done by individual chaperone overproduction or induction of the heat shock
61 response, the mechanism by which *E. coli* naturally responds to misfolded proteins; however, this
62 route is far from generic and needs to be individually tested and optimised for each recombinant
63 protein and host.

64 Another, more generically applicable, approach to increasing recombinant protein folding is
65 minimisation of stress, typified by reducing the rate of recombinant protein production thus allowing
66 recombinant protein translation and folding to proceed more slowly. Examples are the use of *E. coli*
67 strains that transcribe recombinant protein-encoding genes more slowly [11] and reduction of
68 inducer concentration and temperature [20]. In the latter system, two important improvements
69 were made to fermentation conditions using the IPTG-induced pET system [24] in order to produce
70 an aggregation-prone recombinant protein (CheY-GFP) in a soluble form. First, an IPTG

71 concentration of 8 μ M was used instead of 0.5 mM, which decreased the rates of CheY-GFP
72 transcription and translation. Second, a growth temperature of 25 °C was used throughout the
73 process instead of growth at 37 °C before induction of recombinant protein production and 25 °C
74 after induction, in order to slow growth and translation rates and prevent cold shock. Although
75 these alterations decreased the rate of recombinant protein synthesis, the reduction in physiological
76 stress imposed on the bacteria meant that plasmid loss was greatly reduced, so far fewer bacteria
77 were non-productive, and the slower rate of synthesis meant that CheY-GFP could be folded into a
78 soluble form, decreasing IB formation. Overall, this 'improved' protocol resulted in far higher overall
79 recombinant protein yields per unit biomass and higher recombinant protein solubility.

80 In order that such methods are useful industrially, they need to be applied to high cell density
81 fermentation regimes such as fed-batch growth. In this study, we developed high cell density fed-
82 batch fermentations using stress-minimisation methods [20] in order to achieve four aims: high
83 biomass generation; high percentage of productive bacteria; high yield of recombinant protein; and
84 enhanced solubility of the generated recombinant protein. We used flow cytometry (FCM) as a
85 single-cell analysis tool to optimise the fermentations in terms of bacterial physiology and
86 productivity. Protocols were developed that tested industrially-derived semi-defined medium,
87 different carbon sources, and different points of induction of recombinant protein production.

88

89 **MATERIALS AND METHODS**

90 ***Bacterial strains, plasmids and microbiological methods***

91 *Escherichia coli* strain BL21* (DE3) ($F^- ompT hsdS_B (r_B^- m_B^-) gal dcm rne131 \lambda(DE3)$) was used
92 throughout (Invitrogen, Paisley, UK). The recombinant CheY-GFP fusion protein was encoded by the
93 pET20bhc-CheY-GFP plasmid [8,20], comprising the *E. coli cheY* gene fused to *gfp* cloned into

94 pET20bhc [7,27]. The *gfp* gene contains the S65T (maximum λ_{ex} red-shifted to 488 nm) and F64L
95 (folding improvement) mutations and so is equivalent to the GFPmut1 protein [4]. Bacteria were
96 transformed with the plasmid using the heat-shock method and transformants selected on nutrient
97 agar (Oxoid) plates supplemented with 100 μg carbenicillin mL^{-1} (Melford, Ipswich, UK; a more stable
98 variant of ampicillin). Optical density at 650 nm was used as a routine measurement technique for
99 biomass, due to its widespread use industrially and speed of data acquisition. For colony forming
100 unit (CFU) analysis, bacterial cultures were serially decimally diluted in PBS (8 $\text{g}\cdot\text{L}^{-1}$ NaCl, 0.2 $\text{g}\cdot\text{L}^{-1}$ KCl,
101 1.15 $\text{g}\cdot\text{L}^{-1}$ Na_2HPO_4 , 0.2 $\text{g}\cdot\text{L}^{-1}$ KH_2PO_4 , pH 7.3; Oxoid), plated onto nutrient agar plates (Oxoid) and
102 incubated at 25 °C for 48 hours. Colonies were replica plated onto plates containing 80 μg
103 carbenicillin mL^{-1} to determine plasmid retention. The dry cell weight (DCW) of four aliquots of 2 mL
104 of culture (harvested by centrifugation) was determined after drying at 100 °C for ≥ 24 hours.

105 ***Fermentation methods***

106 An Electrolab (Tewkesbury, UK) Fermac 310/60 5 L bioreactor was used with 4 baffles and an
107 agitator with 2 six-bladed Rushton turbines. Aeration was achieved by sparging air from below the
108 lower impeller at a rate of 3 $\text{L}\cdot\text{min}^{-1}$ through a reusable, autoclavable 0.22 μm filter (Sartorius).
109 Dissolved oxygen tension (DOT) was measured *in situ* using a D150 Oxyprobe (Broadley James) and
110 was maintained above a set point of 30% by increasing agitation to a maximum of 1000 RPM from a
111 minimum of 200-500 RPM. pH was measured by an F-695 Fermprobe (Broadley James) and was
112 controlled at a set point of 6.3 ± 0.1 with the automated addition of sterile 10% (v/v) NH_3 or 5% (v/v)
113 HCl. Off gas was passed through a condenser, autoclavable 0.22 μm filter (Sartorius), 2 catch pots
114 and analysed using a PrimaDB gas mass spectrometer (Thermo); data were logged and analysed
115 using GasWorks v1.0 (Thermo).

116 Inocula were grown from a sweep of cells from an agar plate in 35 mL of LB (10 $\text{g}\cdot\text{L}^{-1}$ Tryptone (BD
117 Bacto), 5 $\text{g}\cdot\text{L}^{-1}$ Yeast extract (BD Bacto), 5 $\text{g}\cdot\text{L}^{-1}$ NaCl (Sigma)) supplemented with 100 $\mu\text{g}\cdot\text{mL}^{-1}$

118 carbenicillin in a 250 mL conical flask, at 25°C and agitated at 150 RPM for 18-21 hours. Prior to
119 addition to the vessel, 5 mL of inoculum was removed and used for screening and analysis.

120 Five fermentation protocols were used as outlined in Table 1; the initial batch medium volume was
121 1.5 L in each case. Protocol A used a complex LB-based medium [20]: 10 g·L⁻¹ Tryptone (BD Bacto), 5
122 g·L⁻¹ Yeast extract (BD Bacto), 5 g·L⁻¹ NaCl (Sigma), 1 mL·L⁻¹ *E. coli* sulphur free salts and 1 mL·L⁻¹
123 Silicone antifoam (Corning); supplemented post-autoclaving with 5 g·L⁻¹ glucose and 100 mg·L⁻¹
124 carbenicillin. *E. coli* sulphur-free salts comprised 8.2 g MgCl₂·7H₂O, 1 g MnCl₂·4H₂O, 0.4 g FeCl₃·6H₂O,
125 0.1 g CaCl₂ and 2 mL concentrated HCl in 100 mL of distilled water. CheY-GFP production was
126 induced by the addition of 8 µM IPTG at an OD₆₅₀ of around 0.5. Five hours post-induction, 1 mM
127 Serine, 1 mM Threonine and 1 mM Asparagine were added to the bioreactor. The feed for protocol
128 A contained 100 g·L⁻¹ tryptone, 50 g·L⁻¹ yeast extract, 200 g·L⁻¹ glucose, 10 mM serine, 10 mM
129 threonine, 10 mM asparagine, 100 mg·L⁻¹ carbenicillin, 8µM IPTG, 1 mL·L⁻¹ *E. coli* sulphur-free salts
130 and 0.1% (v/v) silicone antifoam in a final volume of 1 litre. Feeding began on depletion of initial
131 carbon source as indicated by an increase in the DOT (approximately 11 hours post-induction). The
132 feed rate initially was 13.69 mL·h⁻¹ and was increased when on-line monitoring systems (DOT and
133 GC-MS) indicated that the feed rate had become growth-limiting (21.13 mL·h⁻¹ at 30 hours, 27.17
134 mL·h⁻¹ at 44.5 hours and 38.0 mL·h⁻¹ 49.5 hours, feed was exhausted at approximately 57 hours [2]).

135 Protocols B-E used a semi-defined medium [30]: 14 g·L⁻¹ (NH₄)₂SO₄, 20 g·L⁻¹ yeast extract, 2 g·L⁻¹
136 KH₂PO₄, 16.5 g·L⁻¹ K₂HPO₄, 7.5 g·L⁻¹ citric acid, 1.5 mL·L⁻¹ concentrated H₃PO₄ and 0.66 mL·L⁻¹
137 polypropylene glycol as antifoam; supplemented post-autoclaving with 34 mL·L⁻¹ trace metal
138 solution, 10 mM MgSO₄·7H₂O, 2 mM CaCl₂·2H₂O and 100 mg·L⁻¹ carbenicillin. Protocols B-D used 35
139 g·L⁻¹ Glycerol as a carbon source, protocol E used 5 g·L⁻¹ glucose. Trace metal solution contained 3.36
140 g·L⁻¹ FeSO₄·7H₂O, 0.84 g·L⁻¹ ZnSO₄·7H₂O, 0.15 g·L⁻¹ MnSO₄·H₂O, 0.25 g·L⁻¹ Na₂MoO₄·2H₂O, 0.12 g·L⁻¹
141 CuSO₄·5H₂O, 0.36 g·L⁻¹ H₃BO₃ and 48 mL·L⁻¹ concentrated H₃PO₄. The feed composition and rate for

142 protocols B-E are described in Table 1. For protocol D, feeding began prior to depletion of carbon
143 source (17.5 hours post-induction), was paused to allow consumption of glycerol (18.5 hours) and
144 resumed once it was apparent that the glycerol had been consumed (22 hours). For protocol E, an
145 exponential feed profile was calculated using the following equation [23]:

$$F = \left(\frac{1}{S}\right) \times \left(\frac{\mu}{Y_{XS}} + m\right) \times X_0 \times e^{\mu t}$$

146 Where: F equals the feed rate into the bioreactor ($L \cdot h^{-1}$); X_0 , total biomass in bioreactor at start of
147 feed (g dry cell weight); μ , specific growth rate set at 0.2 h^{-1} ; t , time (h); S , feed glucose
148 concentration ($400 \text{ g} \cdot L^{-1}$); Y_{XS} , cell yield on glucose ($0.622 \text{ g biomass} \cdot \text{g glucose}^{-1}$ [28]); and m ,
149 maintenance coefficient for glucose ($0.00468 \text{ g glucose} \cdot \text{g biomass}^{-1} \cdot \text{h}^{-1}$ [28]). A μ of 0.2 was chosen as
150 it is in the range of initial μ values observed (0.05-0.25) for glycerol fermentations in this study.
151 When the feed rate F reached $67.5 \text{ mL} \cdot \text{h}^{-1}$ (at approximately 25.6 hours post-induction), it was not
152 increased any further.

153 **Flow cytometry**

154 Bacteria were analysed using a BD Accuri C6 flow cytometer (BD, Oxford, UK). Samples were excited
155 using a 488 nm solid state laser and fluorescence was detected using 533/30 BP (FL1 channel) and
156 670 LP (FL3 channel) filters corresponding to GFP and propidium iodide (PI) fluorescence
157 respectively. Bacteria were stained with PI to determine viability; PI can only enter dead bacteria. A
158 $200 \mu\text{g PI mL}^{-1}$ stock solution was made up in distilled water and added to samples at a final
159 concentration of $4 \mu\text{g PI mL}^{-1}$. Particulate noise was eliminated using a FSC-H threshold. 20 000 data
160 points were collected at a maximum rate of $2\,500 \text{ events sec}^{-1}$. Data were analysed using CFlow (BD).
161 Percentages of GFP⁺ (productive) bacteria were determined using a gate on a FSC-A versus FL1-A
162 intensity plot. Percentages of PI⁺ (dead) bacteria were determined using a gate on a FL3-A versus
163 FL1-A intensity plot.

164 **SDS-PAGE**

165 Proteins were separated according to molecular weight using Tris/Glycine SDS-PAGE with a 15%
166 (w/v) polyacrylamide gel [18]. Bacterial cell pellets were suspended in sample buffer containing β -
167 mercaptoethanol and heated at 100 °C for 10 minutes before being loaded onto the gel. Equal
168 quantities of biomass were loaded into each lane. SDS-PAGE gels were stained with Coomassie Blue
169 and dried, then scanned (Canon Canoscan 9000F) and the density of each protein band quantified
170 using ImageJ [19] to permit calculation of the percentage of total protein that was CheY-GFP.
171 Independently, soluble and insoluble bacterial protein fractions were separated using BugBuster®
172 (Novagen). Bacterial cell pellets were suspended in a volume of BugBuster® equal to that of sample
173 buffer, incubated at room temperature for 10 minutes then fractionated by centrifugation at 16 873
174 g for 20 min. The pelleted insoluble fraction was subsequently washed in PBS to remove any residual
175 soluble protein. Both fractions were then resuspended in a volume of sample buffer equal to the
176 volume of BugBuster® used and incubated at 100 °C for 10 minutes before separation by SDS-PAGE
177 as above. This protocol results in soluble fractions that are twice the volume and hence half the
178 protein concentration of the insoluble; to ensure gels were loaded with samples from an equivalent
179 biomass twice the volume of soluble fractions were loaded on the gel. ImageJ was used to
180 determine the percentage of CheY-GFP in the soluble and insoluble fractions.

181 **RESULTS AND DISCUSSION**

182 This study investigated the production of the CheY-GFP fusion protein, a model 'difficult' protein
183 that is prone to misfolding and inclusion body formation when overexpressed in *E. coli* [8]. CheY is an
184 *E. coli* chemotaxis protein, and is fused here to the commonly-used *Aequorea victoria* green
185 fluorescent protein (GFP). Previous studies have demonstrated that GFP fluorescence correlates to
186 correct folding of the CheY-GFP fusion, so can be used as a measure of protein solubility and yield
187 [20,27]. The genes encoding CheY-GFP are carried by a pET vector [24]; expression is dependent

188 upon the IPTG-inducible T7 RNA polymerase gene encoded at the DE3 locus of the *E. coli* BL21* host.
189 Initial fermentations followed the ‘improved’ protocol described by Sevastyanovich *et al.* [20],
190 referred to here as protocol A (Table 1). Growth data, measured using optical density at 650 nm,
191 reveal that growth proceeded for 48 hours post-induction (Figure 1a) up to an OD₆₅₀ of around 71.
192 Feeding started 11 hours after induction, triggered by an increase in DOT (Supplemental figure 1)
193 indicating depletion of initial batch phase carbon source (5 g·L⁻¹ glucose). Peak biomass
194 concentration as determined by dry cell weight analysis was 30.1 g·L⁻¹.

195 Plasmid retention as determined by both replica plating and the GFP⁺ phenotype of bacterial
196 colonies on agar plates remained above 94 and 97% respectively (Fig. 1b). We also used flow
197 cytometry (FCM [13]) to determine the green fluorescence of each bacterium; these data are
198 presented as the percentage of bacteria containing GFP (determined by applying a green
199 fluorescence/forward scatter gate, within which bacteria are considered to be GFP⁺) and the mean
200 green fluorescence of GFP⁺ cells, denoted FL1-A (Fig. 1c). The percentage of GFP⁺ cells as determined
201 by FCM remained above 90% (Figure 1b), closely correlating with agar plate data. Less than 5% of
202 bacteria were dead throughout the fermentation as determined by FCM and Propidium Iodide (PI)
203 staining. Online gas MS data (Supplementary Figure 1) reveal that oxygen demand and CO₂ evolution
204 rates dropped sharply after around 55 hours post-induction, corresponding to the end of the feed.

205 The mean green fluorescence of CheY-GFP⁺ bacteria (FL1-A, determined using FCM) increased over
206 the course of the fermentation following a small decrease immediately post-induction (Fig. 1c),
207 thought to be caused by a concurrent decrease in bacterial size (as indicated using FCM forward
208 scatter [FSC-A] measurements). The cell size dynamics observed here are concomitant with previous
209 studies of *E. coli* cell size over growth curves; an increase in cell size during lag phase, followed by a
210 decrease in cell size during exponential growth [1].

211 Maximum green fluorescence per bacterium did not increase significantly after 28 hours post-
212 induction, although biomass increased thus increasing the quantity of recombinant protein present
213 in the fermenter as a whole. SDS-PAGE analysis of whole bacteria and soluble and insoluble bacterial
214 fractions (Fig. 1d) revealed that CheY-GFP concentration per unit biomass (expressed as a
215 percentage of whole cell protein) did not dramatically change during the fermentation, increasing
216 slightly from 11.4 % at induction to 16.8 % at 24 hours post-induction, then fluctuated over the
217 remainder of the fermentation. The percentage of CheY-GFP in the soluble fraction (as determined
218 by Bugbuster® extraction) did increase from around 40% soluble at induction to over 60% soluble 26
219 hours post induction; this increase occurred at the same time as the increase in green fluorescence
220 as measured by FCM.

221 Taken together, the protocol A fermentation could therefore be split into three phases: 0-28 hours
222 post-induction, concurrent increase in biomass and quantity of recombinant protein per cell; 28-48
223 hours, biomass accumulation but no change in quantity of CheY-GFP per cell; and accumulation of
224 neither biomass nor recombinant protein after 48 hours post-induction. 48 hours could be
225 determined to be the optimal harvest time. The final yield of total CheY-GFP produced (at 70 hours
226 post-induction) was estimated to be 2.3 g·L⁻¹ (assuming protein comprises 60 % of dry cell weight,
227 based on observations of 50-61 % [26] and an estimate of 70 % by Sevastyanovich *et al.* [20]),
228 corresponding to a yield of 1.5 g·L⁻¹ soluble CheY-GFP.

229 Three potential problems were identified with protocol A [20] that could limit its utility in
230 biopharmaceutical manufacturing. First, both the base medium and feed contain complex animal-
231 derived products (tryptone) so are not suitable for a cGMP process. Many industrial RPP processes
232 tend to use defined media or semi-defined media without animal products; choice of defined or
233 semi-defined media is usually down to company policy and product. The use of semi-defined media
234 offers a compromise before the potentially high cost of development of a fully defined medium

235 optimised for a particular bioprocess. Minimisation of the use of complex media components also
236 decreases the risks of batch variability. This variability was characterised for this system by growing
237 the *E. coli* BL21* pCheY-GFP strain for 14 hours at 30 °C in LB medium composed of complex medium
238 components sourced from different suppliers: a variability of 21 % in final OD₆₅₀ was observed due to
239 differences in yeast extract and tryptone composition.

240 Second, large quantities of additional complex medium components are fed into the fermenter
241 during the fed-batch phase. This can result in osmotic problems and the presence of large quantities
242 of undefined proteinaceous medium components can complicate downstream processing of product
243 proteins [5]. Finally, use of glucose as a feed can present difficulties from acid formation due to
244 overflow metabolism, especially when growth rates fluctuate. Use of glycerol as a carbon source
245 does not usually present this problem. These three concepts in industrial fermentation design are
246 typified by the protocol used by Want *et al.* [30], which was used to test CheY-GFP expression here
247 (referred to as protocol B; Table 1).

248 ***Use of an industrially-derived fermentation protocol***

249 As well as the use of semi-defined medium and glycerol as carbon source, protocol B used a growth
250 temperature of 37 °C and induction at a relatively high biomass using a high concentration (0.1 mM)
251 of IPTG. The glycerol feed was started at the same time as induction, when online measurements
252 suggested exhaustion of batch-phase glycerol (primarily by reduction in oxygen demand), and was
253 fed at a rate of 67.5 mL·h⁻¹. This protocol resulted in more heterogenous data than protocol A; data
254 from two fermentations are shown in Figure 2. The growth data in terms of OD₆₅₀ and CFU
255 measurements are similar for both fermentations (Fig. 2a). Cell density increased to an OD₆₅₀ of
256 around 55, whereupon RPP was induced by addition of 0.1 mM IPTG. Growth continued until an
257 OD₆₅₀ of around 80; oxygen consumption data (DOT and gas MS) reveal that induction caused
258 growth arrest followed by a recovery, but rapid growth only proceeded for around 5 hours post-

259 induction (Supplementary figure 2). This is indicative of metabolic stress generated upon CheY-GFP
260 synthesis at 37 °C [20].

261 Although the growth of duplicate fermentations was similar, CheY-GFP production in each
262 fermentation was quite different. Both replicates showed high levels of plasmid loss before
263 induction (as determined both by plating and FCM; Figure 2b), suggesting that even uninduced cells
264 were under stress. CheY-GFP is synthesised from this plasmid system even in the absence of inducer
265 (Fig. 1), thus imposing stress before induction [20]. FCM data revealed that 15 hours post-induction,
266 >30% of bacteria were still CheY-GFP⁺ in fermenter 1; despite this, on agar plates, all colonies from
267 fermenter 1 were GFP⁻ at this timepoint. This is likely caused by physiological stress in CheY-GFP⁺
268 bacteria generating a viable but non-culturable (VBNC) phenotype, commonly encountered in
269 bacterial recombinant protein production cultures. Plasmid loss was greater in fermentation 2 than
270 1; only ≈10% of bacteria were CheY-GFP⁺. The proportion of dead (PI⁺) bacteria in fermenter 1 was
271 also higher than in fermenter 2, and the CFU·mL⁻¹ was lower. Mean green fluorescence of the CheY-
272 GFP⁺ bacteria were equivalent (Fig. 2c), but the much lower proportion of productive bacteria in
273 fermenter 2 meant that far less CheY-GFP was produced per unit biomass (Fig. 2d). It is interesting to
274 note that the solubility of CheY-GFP produced by fermenter 2 was very high; this is probably a
275 consequence of the very low quantity of CheY-GFP being produced.

276 For fermenter 1, the final yield of CheY-GFP was estimated at 2.2 g·L⁻¹, corresponding to a yield of
277 0.7 g·L⁻¹ soluble CheY-GFP. It can be concluded that fermenter 1 was more productive in terms of
278 CheY-GFP productivity per unit biomass, but that bacteria were under greater physiological stress.
279 Fermenter 2 had a lower proportion of productive bacteria, resulting in a lower CheY-GFP yield (≈
280 0.6 g·L⁻¹ CheY-GFP, ≈ 0.5 g·L⁻¹ soluble CheY-GFP) but less physiological stress, resulting in higher CFU
281 measurements and a lower proportion of dead bacteria.

282 The low overall levels of plasmid retention, green fluorescence and CheY-GFP accumulation and
283 solubility as compared to protocol A suggests that protocol B put bacteria under physiological stress
284 that was detrimental to recombinant protein production. Therefore, the improvements used to
285 initially design the improved protocol A were applied to the industrially-derived protocol B; namely
286 reduction of temperature to 25 °C throughout and induction with a far lower concentration of IPTG
287 (8 µM) to generate protocol C (Table 1).

288 ***Application of improved conditions to an industrial protocol***

289 Due to the low growth temperature compared to protocol B, protocol C cultures grew far slower
290 (Fig. 3a), taking around 21 hours to reach the induction point ($OD_{650} \approx 40$, when glycerol was
291 exhausted as indicated by online measurements). Following induction, the culture grew well for 11
292 hours as indicated by a steady increase in oxygen demand (DOT and gas MS data; Supplementary
293 figure 3). The feed likely became growth limiting at 11 hours post-induction, even though it lasted
294 until around 18 hours post induction, at which point oxygen demand (as determined by gas MS) fell
295 dramatically. The final OD_{650} was recorded as 297. Unlike protocol B cultures, the proportion of GFP⁺
296 bacteria as measured by FCM remained very high throughout (>93%), indicative of good plasmid
297 retention and a consequence of lowered physiological stress (Fig. 3b). Mean green fluorescence per
298 GFP⁺ bacterium as determined by FCM (FL1-A) decreased between inoculation and induction
299 (concurrent with a decrease in cell size, signified by mean FSC-A measurements) and, as in protocol
300 A, increased following induction, although this increase was to a far greater extent than protocol A
301 cultures, reaching a peak mean green fluorescence of 240 000 compared to 176 000 for protocol A
302 (Fig. 3c). Unlike protocol A cultures, mean forward scatter (FSC-A), signifying bacterial size, increased
303 following induction, and was greater at the end of the fermentation in protocols B and C than in
304 protocol A. This is probably due to the higher osmolarity in the medium and feed used in protocol A
305 [16].

306 CheY-GFP solubility as determined by Bugbuster® peaked at nearly 60% at the point of induction,
307 then decreased to a low point at 5 hours post-induction however recovered to almost the peak value
308 at termination reaching a final solubility of around 56% (Fig. 3d). Total CheY-GFP accumulation per
309 unit biomass followed a similar pattern however peak accumulation occurred at 2 hours post-
310 induction. These data suggest that CheY-GFP concentration per unit biomass and solubility were
311 lowest during periods of rapid growth. The final yield of CheY-GFP was estimated at 10.7 g·L⁻¹,
312 corresponding to a yield of 6 g·L⁻¹ soluble CheY-GFP.

313 Summary data comparing protocols B and C (Table 2) clearly demonstrate the benefits of operating
314 using stress minimisation conditions in terms of the resultant biomass yield (Final OD₆₅₀ increased
315 nearly 4-fold; DCW increased almost 3-fold) and recombinant protein yield and solubility. Compared
316 to protocol A, Protocol C showed an almost 5-fold increase in cell density and although FCM analysis
317 showed similar percentages of GFP⁺ cells, suggesting similar levels of plasmid retention, GFP⁺
318 bacteria in protocol C at harvest were 46 % more fluorescent than in protocol A and showed higher
319 levels of homogeneity as evidenced by the lower CV of the green fluorescence values. CheY-GFP
320 solubility as assessed by BugBuster® fractionation was 11% higher in protocol A than in protocol C;
321 this is in agreement with Moore *et al.* [12] who showed that increasing the concentration of complex
322 media components (tryptone and yeast extract) increased solubility of recombinant T4 dCMP
323 deaminase. However, CheY-GFP concentration as a percentage of total cellular protein in protocol C
324 was almost double that of protocol A; this may partially explain the slightly lower solubility, the
325 higher quantity of CheY-GFP having overwhelmed the bacterial protein folding pathways. These
326 data, combined with the increased biomass, resulted in an over 4-fold increase in CheY-GFP
327 volumetric yield and a 4-fold increase in the volumetric yield of soluble CheY-GFP.

328 ***Alteration of induction point***

329 As in protocol B [30], many RPP protocols induce recombinant protein production at a relatively high
330 biomass in order to separate biomass generation and recombinant protein production stages. This is
331 often done when the recombinant protein in question is a 'toxic' protein, prone to cause host
332 bacteria stress; in addition this can lead to reduction in metabolic burden that can be caused by
333 simultaneous requirements for cellular resources for both biomass and recombinant protein
334 generation. For many recombinant protein production processes, the time from induction to time
335 for harvest is limited (the 'production window') and is governed by the amount of time that the host
336 bacteria can generate recombinant protein without losing viability. Protocol A utilised early
337 induction, using the logic that reduction in stress and lower growth rates would allow bacteria to
338 generate recombinant protein more slowly and thus apportion cellular resources more evenly
339 between biomass and recombinant protein generation. Therefore, protocol C was modified to allow
340 induction at an earlier point ($OD_{650} \approx 0.5$), as in protocol A, to generate protocol D.

341 Cell growth was broadly comparable to protocol C, taking around 40 hours to reach an OD_{650} of 288
342 (Fig. 4a). Online data revealed that metabolic activity declined at 28 hours post-induction
343 (Supplementary Fig. 4), reflecting a decrease in growth rate; as with protocol C, this is probably due
344 to the feed rate limiting growth. The proportion of GFP⁺ cells as determined by FCM (Fig. 4b) during
345 early stages of the fermentation was lower than expected at approximately 80%; however, this was
346 mainly due to non-fluorescent antifoam particulate matter with a similar scatter distribution to
347 bacteria; this particulate noise was visible due to a low cell density at the start of these
348 fermentations. At later points in the fermentation the percentage of GFP⁺ cells remained above 95%
349 but at termination the proportion had dropped to 74%. PI staining also showed an increase in the
350 percentage of dead cells at termination up to 8.8%. These data suggest that by termination the
351 culture had become physiologically stressed. As before, the mean green fluorescence of GFP⁺
352 bacteria and the mean forward scatter initially decreased (Fig 4c); after 18 hours post-induction both
353 parameters steadily increased until termination, FL1-A reaching a final value of 370 000. The

354 increase in FL1-A during the latter stages of the fermentation was greater than that of FSC-A
355 (signifying cell size), suggesting accumulation of CheY-GFP per bacterium. FSC-A changes were
356 similar to protocol C, except that induction occurred at the maximum mean FSC-A value rather than
357 the minimum; this suggests that bacterial size is primarily regulated in response to growth phase and
358 is not a result of recombinant protein production. SDS-PAGE analysis (Figure 4d) showed a steady
359 increase in the percentage of total cellular protein that was CheY-GFP throughout; from 16% at the
360 point of induction to 26% at termination. However the percentage solubility showed an overall
361 decrease during the fermentation from 47% at induction to 37% at termination, suggesting that
362 overall product quality had decreased; again, possibly due to higher rates of CheY-GFP synthesis, as
363 seen in protocol C. Final yield of CheY-GFP was estimated at $12 \text{ g}\cdot\text{L}^{-1}$, corresponding to a yield of 4.5
364 $\text{g}\cdot\text{L}^{-1}$ soluble CheY-GFP.

365 Comparing protocols C and D allow the effect of early versus late induction to be examined. In terms
366 of biomass generation protocols C and D showed similar final measurements (Table 2). In addition,
367 culture viability, as indicated by the percentage of PI^+ cells, was similar. It can therefore reasonably
368 be concluded that culture growth and biomass generation did not appear to be affected by earlier
369 induction. In terms of CheY-GFP productivity the effect of early induction was an increase in
370 heterogeneity within the culture. The percentage of total protein that was CheY-GFP was similar at
371 harvest, but the product quality, as indicated by CheY-GFP solubility, was almost 20% lower in
372 protocol D. The proportion of GFP^+ cells was over 20% lower for protocol D, but the mean green
373 fluorescence of the GFP^+ cells was over 50% higher. Nonetheless, similar amounts of CheY-GFP per
374 unit biomass were observed by SDS-PAGE in protocols C and D, although its solubility was lower in
375 protocol D.

376 Based on these data, earlier induction increased culture heterogeneity in protocol D, evidenced by a
377 larger number of GFP^- cells, and a lower percentage of soluble CheY-GFP as determined by SDS-

378 PAGE. It is possible that induction of RPP tends to select for culture heterogeneity, even in stress-
379 minimising conditions; the longer time between induction and harvest allowed a larger
380 subpopulation to develop in protocol D than C. This represents an additional factor when choosing a
381 harvest window.

382 ***Use of glucose as a carbon source***

383 Although glycerol has advantages over glucose as a carbon source, it is more expensive and the
384 preferred carbon and energy source of *E. coli* is glucose. Therefore, protocol D was modified to use
385 glucose as a carbon source both in the batch medium and the feed, generating protocol E. Growth
386 data reveal steady growth to a final OD₆₅₀ of 167 (Fig. 5a); gas MS revealed that growth significantly
387 slowed at 32 hours post-induction (Supplemental Figure 5), corresponding to the end of the glucose
388 feed. Plasmid retention remained above 92% throughout (Fig. 5b). The percentage of GFP⁺ cells
389 determined by FCM remained above 98%, except for the initial sample that was 85%, again caused
390 by antifoam particulates. The percentage of dead cells as determined by FCM remained at less than
391 7% throughout, although there was an increase between 26 hours (1.8%) and termination (5.9%),
392 possibly suggesting a increase in cell stress due to the onset of stationary phase.

393 Mean green fluorescence and forward scatter of GFP⁺ cells (Fig. 5c) showed a similar pattern to
394 other early-induced fermentations. Between 6 and 20 hours post-induction FSC-A decreased to a
395 greater extent than FL1-A, suggesting that while the cells became smaller, CheY-GFP content per cell
396 increased. Between 20 and 26 hours post-induction FL1-A increased by approximately 30% and FSC-
397 A increased by approximately 20%, suggesting accumulation of CheY-GFP per cell despite increasing
398 cell size. At termination mean green fluorescence per bacterium had reached 296 000. SDS-PAGE
399 data (Figure 5d) showed an increase in the percentage of total cellular protein that was CheY-GFP
400 from 2 hours post-induction until termination, reaching a final peak value of 30%. CheY-GFP
401 solubility fluctuated during the fermentation, the peak solubility of 50% being observed at 5 hours

402 post-induction and final solubility being 46%. Final yield of CheY-GFP was estimated at $7.7 \text{ g}\cdot\text{L}^{-1}$,
403 corresponding to a yield of $3.8 \text{ g}\cdot\text{L}^{-1}$ soluble CheY-GFP.

404 Although utilising the same carbon source, protocol E shows several benefits over protocol A: a 2.5-
405 fold increase in OD_{650} ; a 65% increase in the mean green fluorescence of GFP^+ bacteria; and the
406 largest amount of CheY-GFP as expressed as a percentage of cellular protein achieved in this study.

407 Although the soluble percentage of CheY-GFP was higher in protocol A than E, the far higher
408 quantity of CheY-GFP per cell and higher biomass concentration meant that the volumetric yield of
409 soluble CheY-GFP in protocol E was over double that of protocol A ($3.8 \text{ g}\cdot\text{L}^{-1}$ versus $1.5 \text{ g}\cdot\text{L}^{-1}$). As
410 before, increases in CheY-GFP per cell probably correlate with decreases in CheY-GFP solubility due
411 to overloading of cellular protein folding pathways.

412 Comparison of protocols E and D allows elucidation of differences caused by changing carbon
413 source. There are numerous studies that claim recombinant protein production is enhanced by
414 growth on either glucose [3,25] or glycerol [9,15,31]; this seems to be dependent upon recombinant
415 protein, strain, medium composition and growth conditions, and so is likely not a generic effect. In
416 this study, protocol E had a lower final OD_{650} than D; however, this was expected as total glucose
417 added was less than glycerol, and $Y_{x/s}$ values were broadly comparable (Table 2). FCM data
418 demonstrate that there were fewer GFP^- bacteria in protocol E than D, suggesting lower
419 physiological stress, although protocol D had a longer runtime than E, which could select for a non-
420 productive GFP^- subpopulation. CheY-GFP yield per cell and solubility were higher in protocol E,
421 although the higher biomass generated in protocol D resulted in a higher overall CheY-GFP yield.
422 Again, there is a balance between biomass production, CheY-GFP production and solubility;
423 protocols C-E have demonstrated that although each of these parameters may be optimised
424 individually, it is at the expense of other parameters.

425 **CONCLUSIONS**

426 The stress minimisation method [20] has been shown to be highly applicable to an industrially-
427 derived high cell density fed-batch recombinant protein production protocol, both with early and
428 late induction of RPP and with glucose and glycerol as carbon sources. Stress minimisation increased
429 biomass yield and CheY-GFP yield and solubility while decreasing culture heterogeneity. Similarly,
430 transfer to a semi-defined medium improved biomass yield and overall CheY-GFP productivity per
431 unit volume, while representing a more industrially-favoured approach to RPP due to elimination of
432 animal-derived products and minimisation of complex media components. Changing the point of
433 induction was shown to have little overall effect on the improved protocols. Flow cytometry was
434 shown to be a very useful analytical tool in fermentation monitoring and optimisation, in particular
435 allowing culture heterogeneity, stress and the relationship between bacterial size and GFP content
436 to be monitored. In summary, the stress minimisation methods described here could effectively be
437 applied to a wide range of high cell density culture recombinant protein production fermentations.

438 **ACKNOWLEDGEMENTS**

439 This work was supported by a UK Biotechnology and Biological Sciences Research Council PhD
440 studentship to CW. We thank Yanina Sevastyanovich and Tania Selas Castiñeiras for helpful
441 comments on the manuscript.

442 **CONFLICT OF INTEREST STATEMENT**

443 The BD Accuri C6 flow cytometer was awarded to TWO by the BD Accuri Creativity Award. TWO was
444 paid speakers expenses by BD for speaking at a BD Accuri users' event. The funders played no role in
445 the design or implementation of this study.

446 **REFERENCES**

- 447 1. Åkerlund T, Nordström K, Bernander R (1995) Analysis of cell size and DNA content in
448 exponentially growing and stationary-phase batch cultures of *Escherichia coli*. J Bacteriol 177:
449 6791–6797
- 450 2. Alfasi S, Sevastyanovich Y, Zaffaroni L, Griffiths L, Hall R, Cole J (2011) Use of GFP fusions for
451 the isolation of *Escherichia coli* strains for improved production of different target recombinant
452 proteins. J Biotechnol 156: 11-21.
- 453 3. Carvalho RJ, Cabrera-Crespo J, Tanizaki MM, Goncalves VM (2012) Development of production
454 and purification processes of recombinant fragment of pneumococcal surface protein A in
455 *Escherichia coli* using different carbon sources and chromatography sequences. Appl Microbiol
456 Biotechnol 94: 683-94.
- 457 4. Cormack BP, Valdivia RH, Falkow S (1996) FACS-optimized mutants of the green fluorescent
458 protein (GFP). Gene. 173: 33-8.
- 459 5. Cote RJ (2010) Media composition, microbial, laboratory scale. In: Encyclopedia of Industrial
460 Biotechnology, Bioprocess, Bioseparation, and Cell Technology. Flickinger MC, ed. John Wiley &
461 Sons. pp 3277-3297
- 462 6. García-Fruitós E, González-Montalbán N, Morell M, Vera A, Ferraz RM, Arís A, Ventura S,
463 Villaverde A (2005) Aggregation as bacterial inclusion bodies does not imply inactivation of
464 enzymes and fluorescent proteins. Microb Cell Fact 4: 27
- 465 7. Jones JJ, Bridges AM, Fosberry AP, Gardner S, Lowers RR, Newby RR, James PJ, Hall RM, Jenkins
466 O (2004) Potential of real-time measurement of GFP-fusion proteins. J Biotechnol 109: 201-11
- 467 8. Jones JJ (2007) Green fluorescent protein as an analytical tool to dissect the physiology of
468 recombinant protein production in fermenters. PhD thesis, University of Birmingham,
469 Birmingham, UK.
- 470 9. Luo Q, Shen YL, Wei DZ, Cao W (2006) Optimization of culture on the overproduction of TRAIL in
471 high-cell-density culture by recombinant *Escherichia coli*. Appl Microbiol Biotechnol 71: 184-91.

- 472 10. Martínez-Alonso M, García-Fruitós E, Ferrer-Miralles N, Rinas U, Villaverde A (2010) Side effects
473 of chaperone gene co-expression in recombinant protein production. *Microb Cell Fact* 9: 64.
- 474 11. Miroux, B and Walker, JE (1996) Over-production of proteins in *Escherichia coli*: mutant hosts
475 that allow synthesis of some membrane proteins and globular proteins at high levels. *J Mol Biol*
476 260: 289-98.
- 477 12. Moore JT, Uppal A, Maley F, Maley GF (1993) Overcoming inclusion body formation in a high-
478 level expression system. *Protein Expr Purif* 4: 160-3.
- 479 13. Müller S, Nebe-von-Caron G (2010) Functional single-cell analyses: flow cytometry and cell
480 sorting of microbial populations and communities. *FEMS Microbiol Rev* 34: 554-87.
- 481 14. Overton TW (2014) Recombinant protein production in bacterial hosts. *Drug Discov Today In*
482 *press* doi:10.1016/j.drudis.2013.11.008
- 483 15. Pflug, S, Richter, S M & Urlacher, V B (2007) Development of a fed-batch process for the
484 production of the cytochrome P450 monooxygenase CYP102A1 from *Bacillus megaterium* in *E.*
485 *coli*. *J Biotechnol* 129: 481-8.
- 486 16. Reuter M, Hayward NJ, Black SS, Miller S, Dryden DT, Booth IR (2013) Mechanosensitive
487 channels and bacterial cell wall integrity: does life end with a bang or a whimper? *J R Soc*
488 *Interface*. 11: 20130850. doi: 10.1098/rsif.2013.0850.
- 489 17. Saïda F, Uzan M, Odaert B, Bontems F (2006) Expression of highly toxic genes in *E. coli*: special
490 strategies and genetic tools. *Curr Protein Pept Sci* 7: 47-56.
- 491 18. Sambrook J, Fritsch EF, Maniatis T (1987) *Molecular Cloning: A Laboratory Manual*, 2nd edn.
492 Cold Spring Harbor Press, Cold Spring Harbor, NY.
- 493 19. Schneider CA, Rasband WS, Eliceiri KW (2012) NIH Image to ImageJ: 25 years of image analysis.
494 *Nat Methods* 9: 671-675.

- 495 20. Sevastyanovich Y, Alfasi S, Overton T, Hall R, Jones J, Hewitt C, Cole J (2009) Exploitation of GFP
496 fusion proteins and stress avoidance as a generic strategy for the production of high-quality
497 recombinant proteins. *FEMS Microbiol Lett* 299: 86–94.
- 498 21. Singh, SM and Panda, AK (2005) Solubilization and refolding of bacterial inclusion body proteins.
499 *J Biosci Bioeng* 99: 303-10.
- 500 22. Sørensen HP, Mortensen KK. (2005) Soluble expression of recombinant proteins in the
501 cytoplasm of *Escherichia coli*. *Microb Cell Fact.* 4: 1.
- 502 23. Strandberg, L, Andersson, L, Enfors, S (1994) The use of fed batch cultivation for achieving high
503 cell densities in the production of a recombinant protein in *Escherichia coli*. *FEMS Microbiol Rev*
504 14: 53–6.
- 505 24. Studier FW(1991) Use of bacteriophage T7 lysozyme to improve an inducible T7 expression
506 system. *J Mol Biol* 219: 37-44.
- 507 25. Tseng, C L & Leng, C H (2012) Influence of medium components on the expression of
508 recombinant lipoproteins in *Escherichia coli*. *Appl Microbiol Biotechnol* 93: 1539-52.
- 509 26. Valgepea, K, Adamberg, K, Seiman, A, Vilu, R (2013) *Escherichia coli* achieves faster growth by
510 increasing catalytic and translation rates of proteins. *Mol Biosyst* 9: 2344-58.
- 511 27. Waldo GS, Standish BM, Berendzen J, Terwilliger TC (1999) Rapid protein-folding assay using
512 green fluorescent protein. *Nat Biotechnol* 17: 691-5.
- 513 28. Wallace, R, Holms, W (1986) Maintenance coefficients and rates of turnover of cell material in
514 *Escherichia coli* ML308 at different growth temperatures. *FEMS Microbiol Lett* 37: 317-320
- 515 29. Walsh G (2010) Biopharmaceutical benchmarks. *Nat. Biotechnol* 28: 917-24.
- 516 30. Want A, Thomas OR, Kara B, Liddell J, Hewitt CJ. (2009) Studies related to antibody fragment
517 (Fab) production in *Escherichia coli* W3110 fed-batch fermentation processes using
518 multiparameter flow cytometry. *Cytometry A* 75: 148-54.

519 31. Zhang JD, Li AT, Xu JH (2010) Improved expression of recombinant cytochrome P450
520 monooxygenase in *Escherichia coli* for asymmetric oxidation of sulfides. *Bioprocess Biosyst Eng*
521 33: 1043-9.

522

523 **FIGURE LEGENDS**

524 **Figure 1.** Fermentation data using protocol A (Original ‘improved’ protocol, complex medium and
525 feed, early induction). A. OD₆₅₀ (squares) and CFU (crosses) data. Arrow indicates time of feed
526 starting. B. Plasmid retention data; percentage of colonies that were GFP⁺ (squares) and percentage
527 plasmid⁺ colonies (crosses) as determined using agar plates. Flow cytometry data; percentage of
528 cells that were GFP⁺ (circles) and percentage of cells that were PI⁺ and so dead (triangles). C. Flow
529 cytometry data; mean cellular green fluorescence (FL1-A) of GFP⁺ cells (squares) and mean forward
530 scatter (FSC-A) of GFP⁺ cells (crosses). D. SDS-PAGE data; percentage solubility of CheY-GFP (squares)
531 and percentage of total protein that was CheY-GFP (crosses). Data from a representative
532 fermentation of a minimum of 2 replicates.

533 **Figure 2.** Fermentation data using protocol B (Industrially derived ‘standard’ conditions, semi-
534 defined medium, late induction, high [IPTG]). A - OD₆₅₀ data for replicate 1 (squares) and 2 (crosses)
535 CFU data for replicate 1 (circles) and 2 (triangles). Arrow indicates time of feed starting. B - Plasmid
536 retention data; percentage of colonies that were GFP⁺ (squares) and percentage plasmid⁺ colonies
537 (crosses) as determined using agar plates. Flow cytometry data; percentage of cells that were GFP⁺
538 (circles) and percentage of cells that were PI⁺ and so dead (triangles). Replicate 1 – left, replicate 2 –
539 right. C - Flow cytometry data; mean cellular green fluorescence (FL1-A) of GFP⁺ cells (squares) and
540 mean forward scatter (FSC-A) of GFP⁺ cells (crosses). Replicate 1 – left, replicate 2 – right. D - SDS-
541 PAGE data; percentage solubility of CheY-GFP (squares) and percentage of total protein that was
542 CheY-GFP (crosses). Replicate 1 – left, replicate 2 – right.

543 **Figure 3.** Fermentation data using protocol C (Improved industrially derived conditions, semi-defined
544 medium, late induction, low [IPTG]). A. OD₆₅₀ (squares) and CFU (crosses) data. Arrow indicates time
545 of feed starting. B. Flow cytometry data; percentage of cells that were GFP⁺ (squares) and
546 percentage of cells that were PI⁺ and so dead (crosses). C. Flow cytometry data; mean cellular green
547 fluorescence (FL1-A) of GFP⁺ cells (squares) and mean forward scatter (FSC-A) of GFP⁺ cells (crosses).
548 D. SDS-PAGE data; percentage solubility of CheY-GFP (squares) and percentage of total protein that
549 was CheY-GFP (crosses). Data from a representative fermentation of a minimum of 2 replicates.

550 **Figure 4.** Fermentation data using protocol D (Improved industrially derived conditions, semi-
551 defined medium, early induction, low [IPTG]). A. OD₆₅₀ (squares) data. Arrow indicates time of feed
552 starting. B. Flow cytometry data; percentage of cells that were GFP⁺ (squares) and percentage of
553 cells that were PI⁺ and so dead (crosses). C. Flow cytometry data; mean cellular green fluorescence
554 (FL1-A) of GFP⁺ cells (squares) and mean forward scatter (FSC-A) of GFP⁺ cells (crosses). D. SDS-PAGE
555 data; percentage solubility of CheY-GFP (squares) and percentage of total protein that was CheY-GFP
556 (crosses). Data from a representative fermentation of a minimum of 2 replicates.

557 **Figure 5.** Fermentation data using protocol E (Improved industrially derived conditions, semi-defined
558 medium, early induction, low [IPTG], glucose feed). A. OD₆₅₀ (squares) and CFU (crosses) data. Arrow
559 indicates time of feed starting. B. Plasmid retention data; percentage of colonies that were GFP⁺
560 (squares) and percentage plasmid⁺ colonies (crosses) as determined using agar plates. Flow
561 cytometry data; percentage of cells that were GFP⁺ (circles) and percentage of cells that were PI⁺ and
562 so dead (triangles). C. Flow cytometry data; mean cellular green fluorescence (FL1-A) of GFP⁺ cells
563 (squares) and mean forward scatter (FSC-A) of GFP⁺ cells (crosses). D. SDS-PAGE data; percentage
564 solubility of CheY-GFP (squares) and percentage of total protein that was CheY-GFP (crosses). Data
565 from a representative fermentation of a minimum of 2 replicates.

	A – Original improved protocol	B – Industrially derived, standard conditions	C – Industrially derived, improved conditions	D – Industrially derived, improved conditions, mid logarithmic induction, glycerol	E – Industrially derived, improved conditions, mid logarithmic induction, glucose
Growth medium	Complex [20]	Semi-defined [30]	Semi-defined [30]	Semi-defined [30]	Semi-defined [30]
Carbon source in batch phase	5 g·L ⁻¹ glucose	35 g·L ⁻¹ glycerol	35 g·L ⁻¹ glycerol	35 g·L ⁻¹ glycerol	5 g·L ⁻¹ glucose
Feed composition and volume	1 L; 100 g·L ⁻¹ Tryptone 50 g·L ⁻¹ Yeast extract 200 g·L ⁻¹ Glucose 10 mM each serine, threonine, asparagine 100 mg·L ⁻¹ carbenicillin, 8 μM IPTG, 1 mL·L ⁻¹ <i>E. coli</i> sulphur-free salts 0.1% (v/v) silicone antifoam	0.5 L 714 g·L ⁻¹ glycerol 7.4 g·L ⁻¹ MgSO ₄ ·7H ₂ O	0.5 L 714 g·L ⁻¹ glycerol 7.4 g·L ⁻¹ MgSO ₄ ·7H ₂ O	0.5 L 714 g·L ⁻¹ glycerol 7.4 g·L ⁻¹ MgSO ₄ ·7H ₂ O	0.5 L 400 g·L ⁻¹ glucose 7.4 g·L ⁻¹ MgSO ₄ ·7H ₂ O
Feed rate	Stepped (<i>see Methods</i>)	67.5 mL·h ⁻¹	67.5 mL·h ⁻¹	67.5 mL·h ⁻¹	Exponential at μ = 0.2, up to 67.5 mL·h ⁻¹
Feed start	On glucose exhaustion	OD ₆₅₀ ≈ 40-50	OD ₆₅₀ ≈ 40-50	On glycerol exhaustion	On glucose exhaustion
Temperature	25°C	37°C	25°C	25°C	25°C
[IPTG]	8 μM	100 μM	8 μM	8 μM	8 μM
Induction point	Mid-logarithmic phase (OD ₆₅₀ ≈ 0.5)	With feeding (OD ₆₅₀ ≈ 40-50)	With feeding (OD ₆₅₀ ≈ 40-50)	Mid-logarithmic phase (OD ₆₅₀ ≈ 0.5)	Mid-logarithmic phase (OD ₆₅₀ ≈ 0.5)

Table 1: Summary of fermentation protocols

Protocol	Peak / final ^a OD ₆₅₀	DCW (g·L ⁻¹)	Y _{xs} (g·g ⁻¹)	Flow cytometry measurements						SDS-PAGE		Total CheY::GFP (g·L ⁻¹) ^c	Total soluble CheY::GFP (g·L ⁻¹)
				% bacteria GFP ⁺	% bacteria PI ⁺	Mean FL1-A (GFP ⁺ bacteria)	Mean FL1-A (all bacteria)	% CV (Coefficient of Variation) FL1-A	Mean FSC-A (GFP ⁺ bacteria)	% CheY::GFP soluble	% of protein that is CheY::GFP		
A	64.5 (71.8)	30.1	0.363	94.3	2.1	166 700 (176 100)	157 200	73	8 800	62.5	13.0	2.3	1.5
B ^b	72.4 (81.8)	27.9	0.136	33.0	6.7	117 700 (117 800)	62 800	93	29 100	30.0	13.4	2.2	0.7
C	297	72.8	0.365	95.2	9.3	240 100	228 600	54	23 900	55.6	24.5	10.7	6
D	288	77.5	0.378	73.5	8.8	369 400	271 600	83	25 200	37.4	25.7	12.0	4.5
E	167	42.6	0.411	98.2	5.9	295 500	290 100	73	22 700	49.5	30.1	7.7	3.8

Table 2. Summary of fermentation data at harvest.

^a Values in parentheses are peak measurements.

^b Values refer to fermentation 1 (Fig. 2)

^c Estimated from DCW and % CheY::GFP of total protein assuming protein comprises 60% of *E. coli* dry cell mass (based on 50-61% estimates from [26] and 70% from [20]).

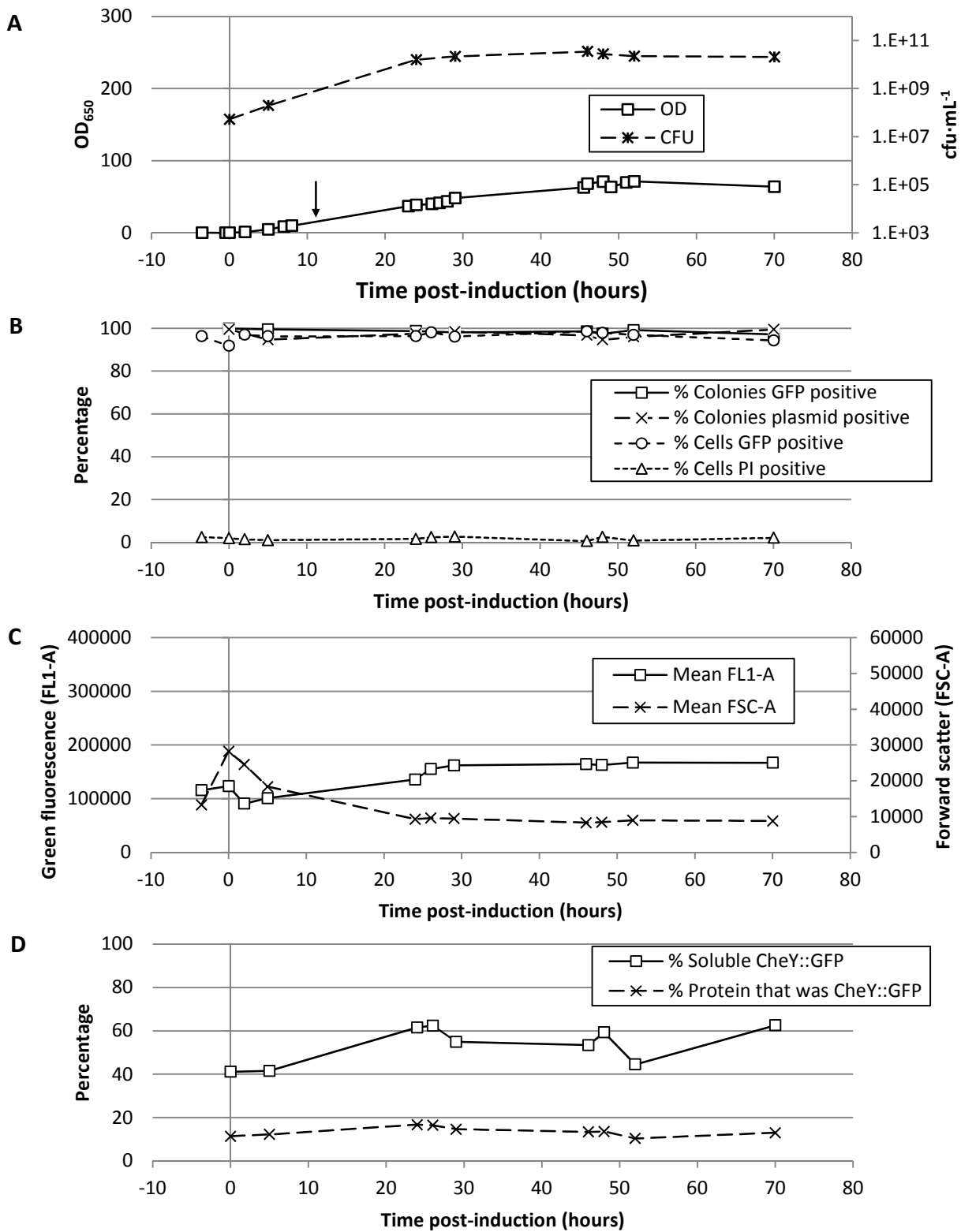


Figure 1

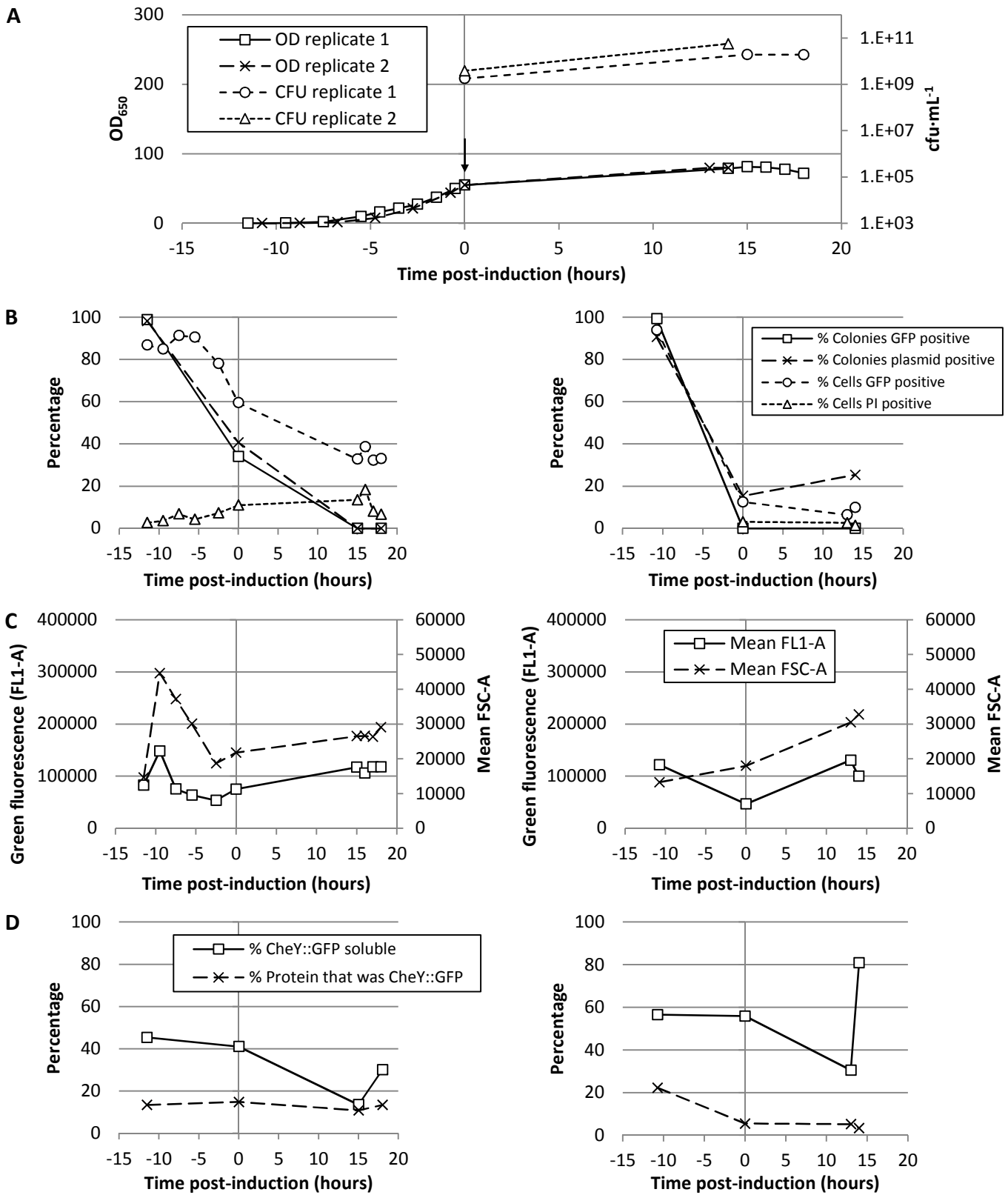


Figure 2

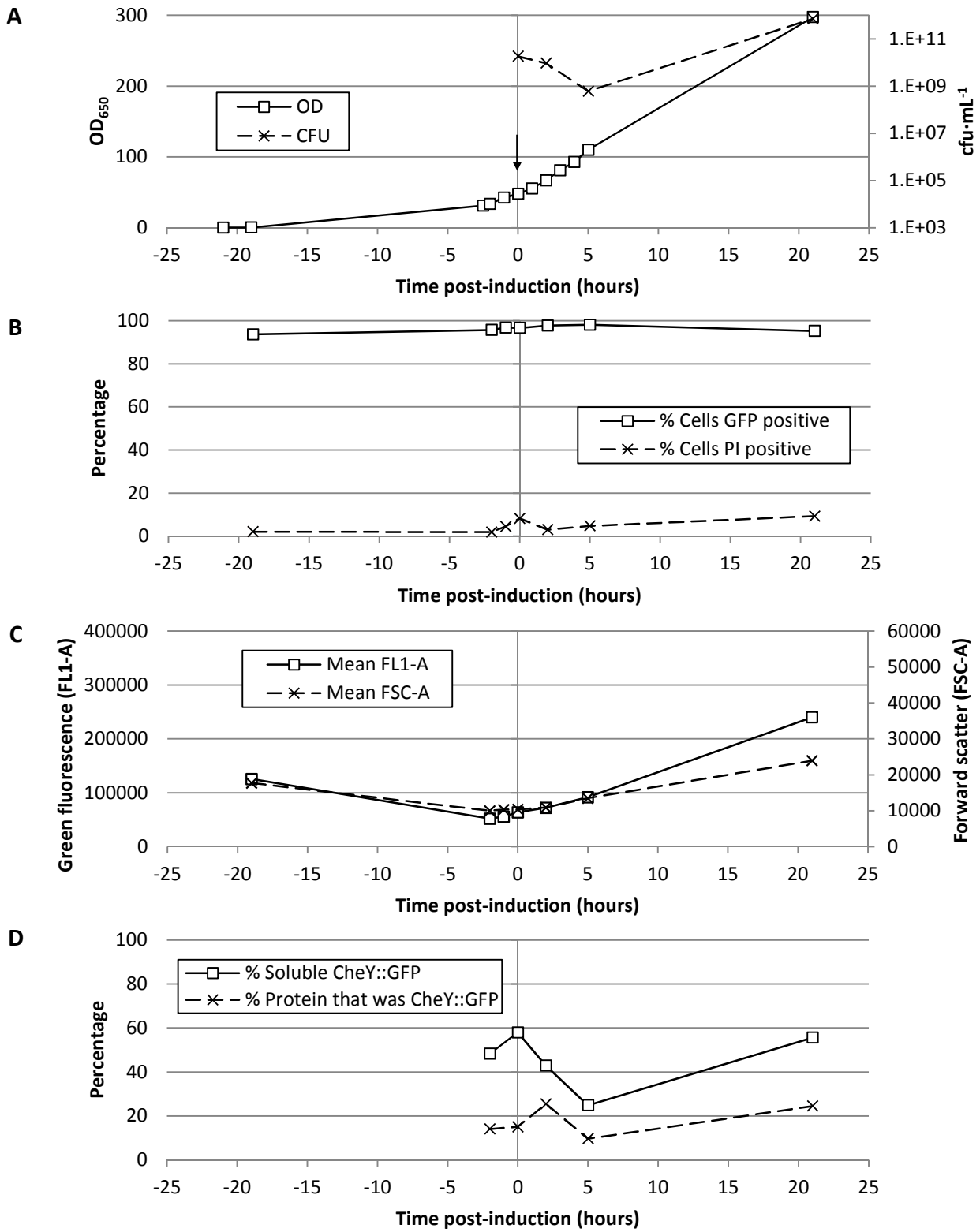


Figure 3

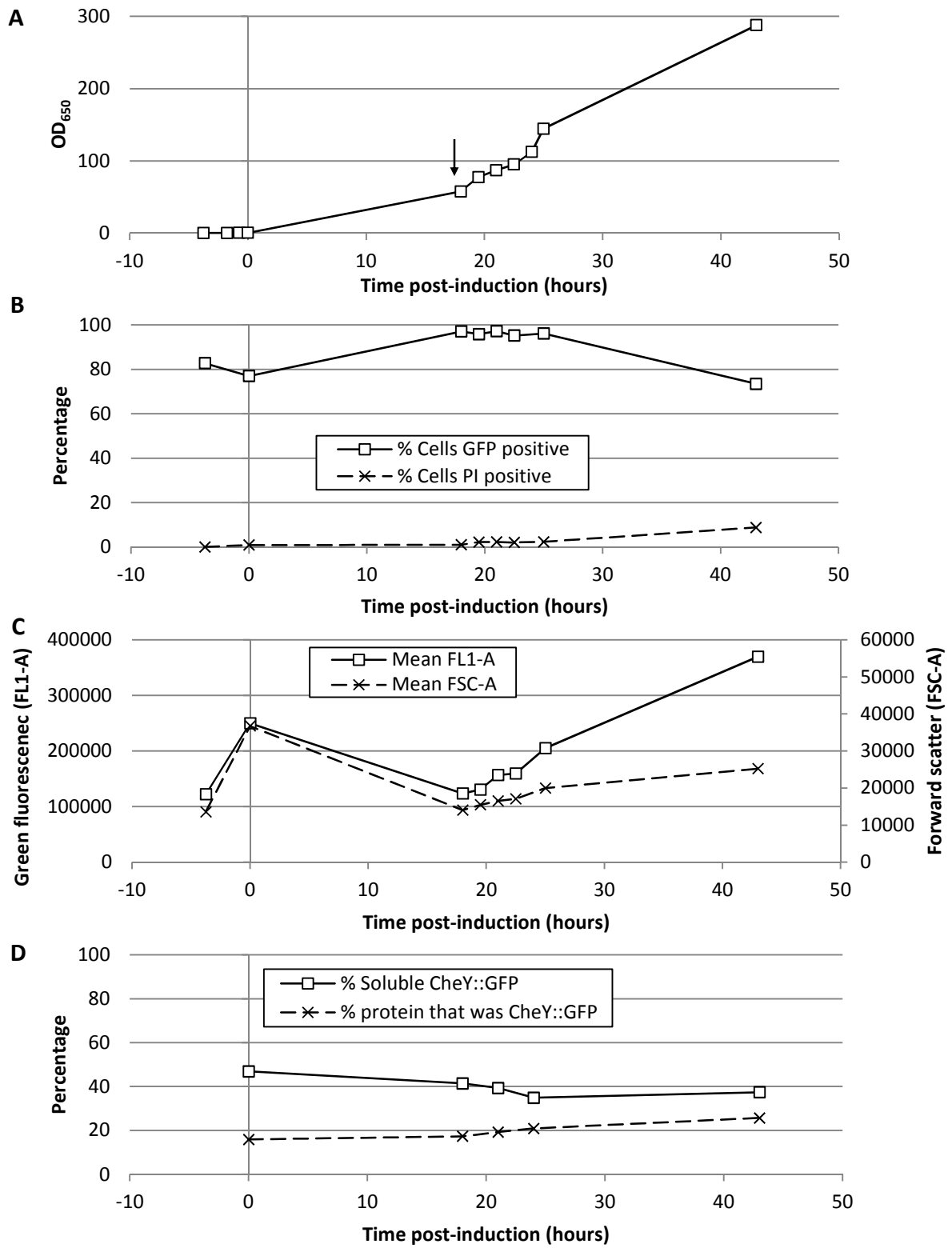


Figure 4

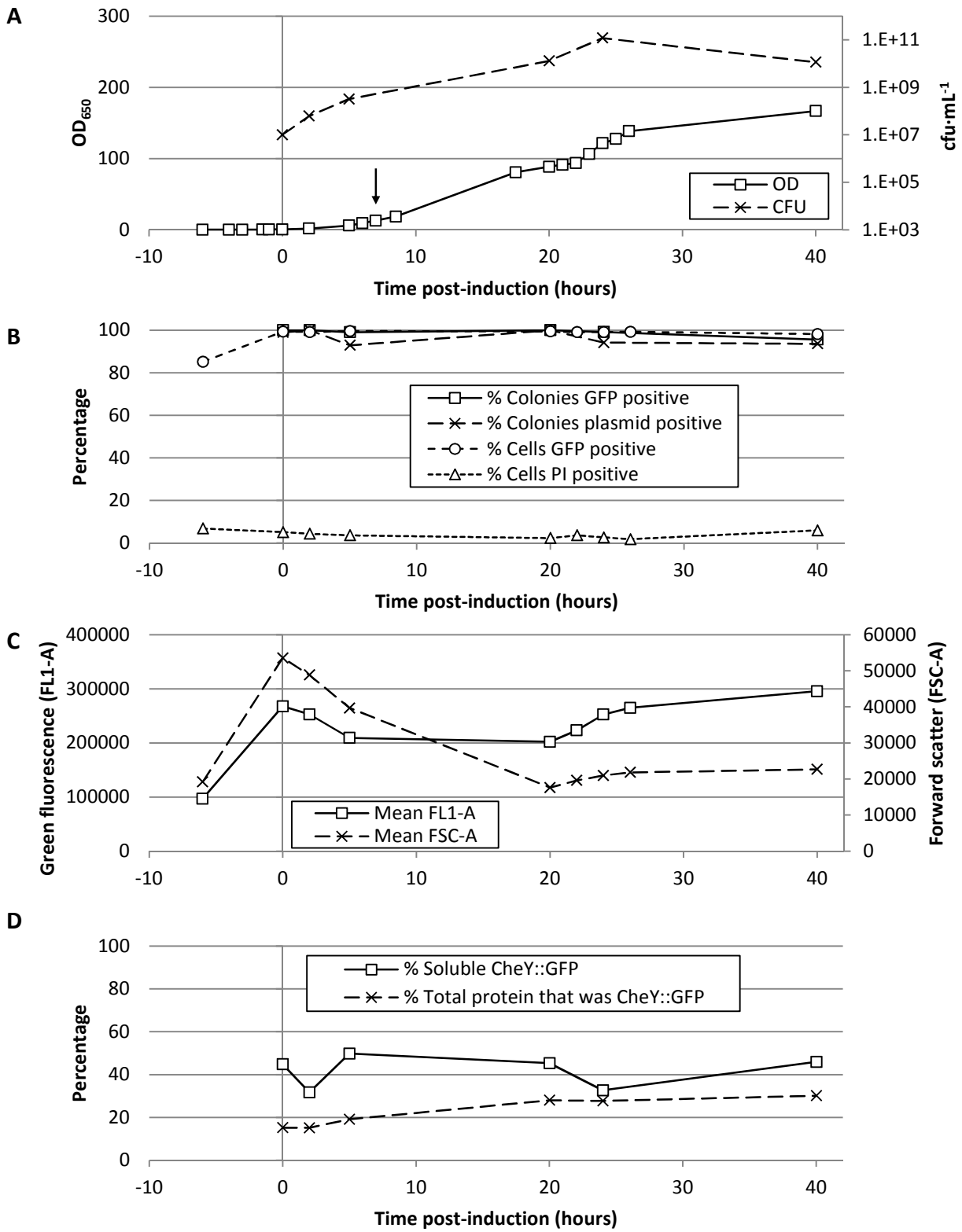


Figure 5

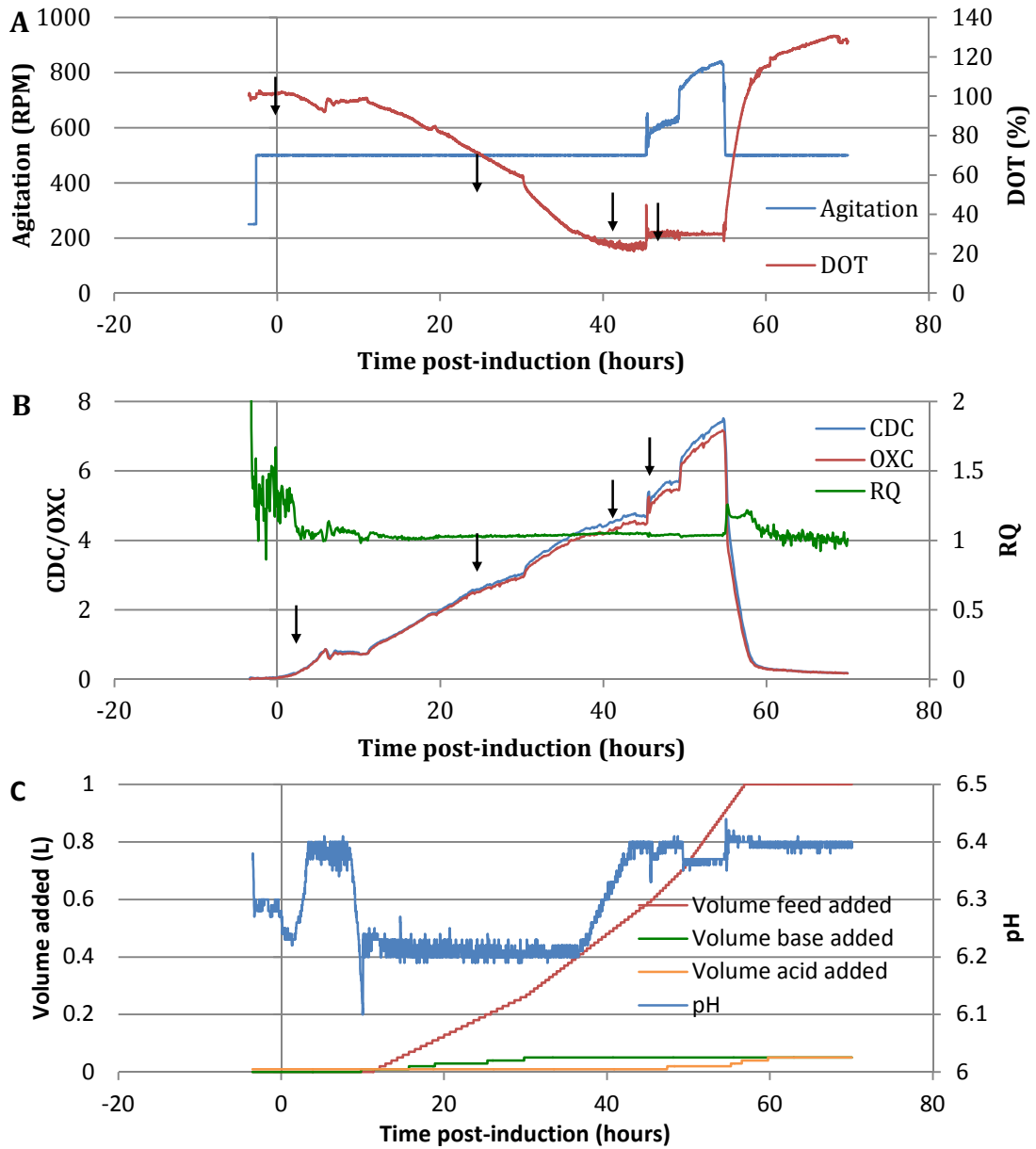
Use of a stress-minimisation paradigm in high cell density fed-batch *Escherichia coli* fermentations to optimise recombinant protein folding

Chris Wyre and Tim W Overton*

Bioengineering, School of Chemical Engineering, and Institute of Microbiology & Infection, University of Birmingham, Edgbaston, Birmingham B15 2TT, UK

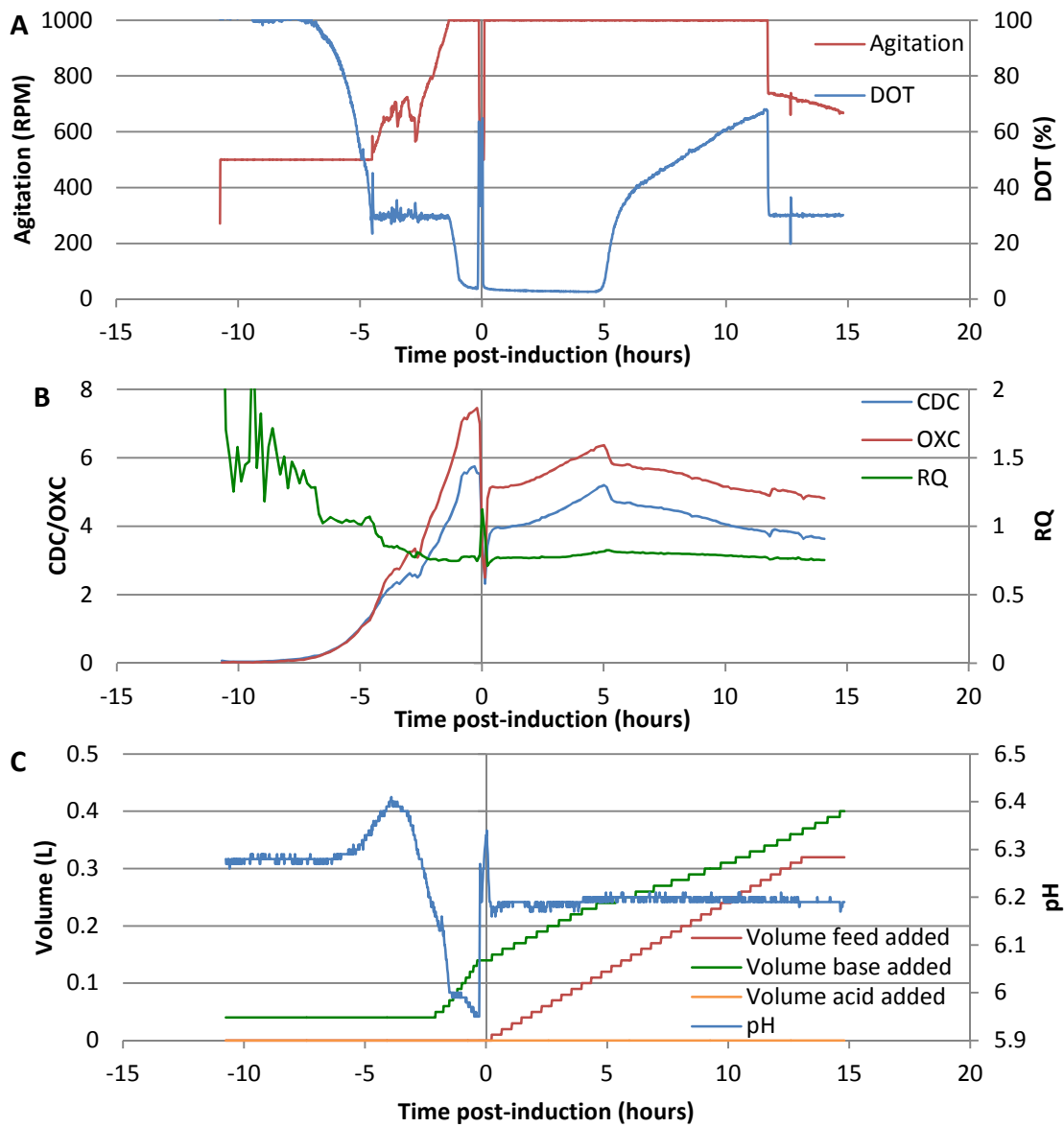
*Corresponding author: t.w.overton@bham.ac.uk

Supplemental Figures 1 - 5



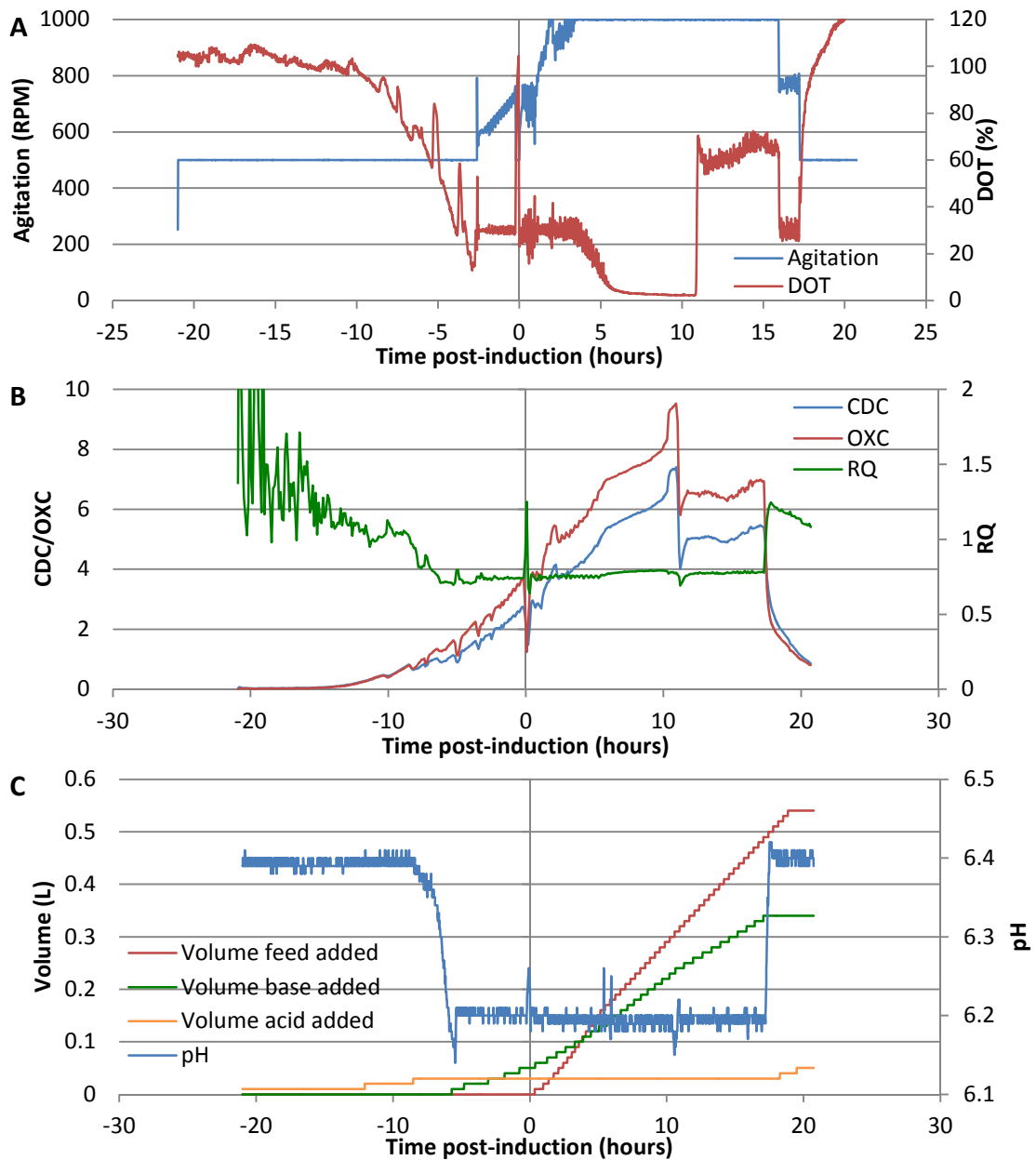
Supplemental figure 1. On-line data from a protocol A fermentation.

A - Agitation (blue) and DOT (red) data. B - Gas-MS data; CDC (blue) OXC (red), RQ (green). C - pH (blue), volumes of feed (red), base (green) and acid (orange) added to vessel. Arrows indicate points at which feed rate was increased, data from a representative fermentation of a minimum of 2 replicates.



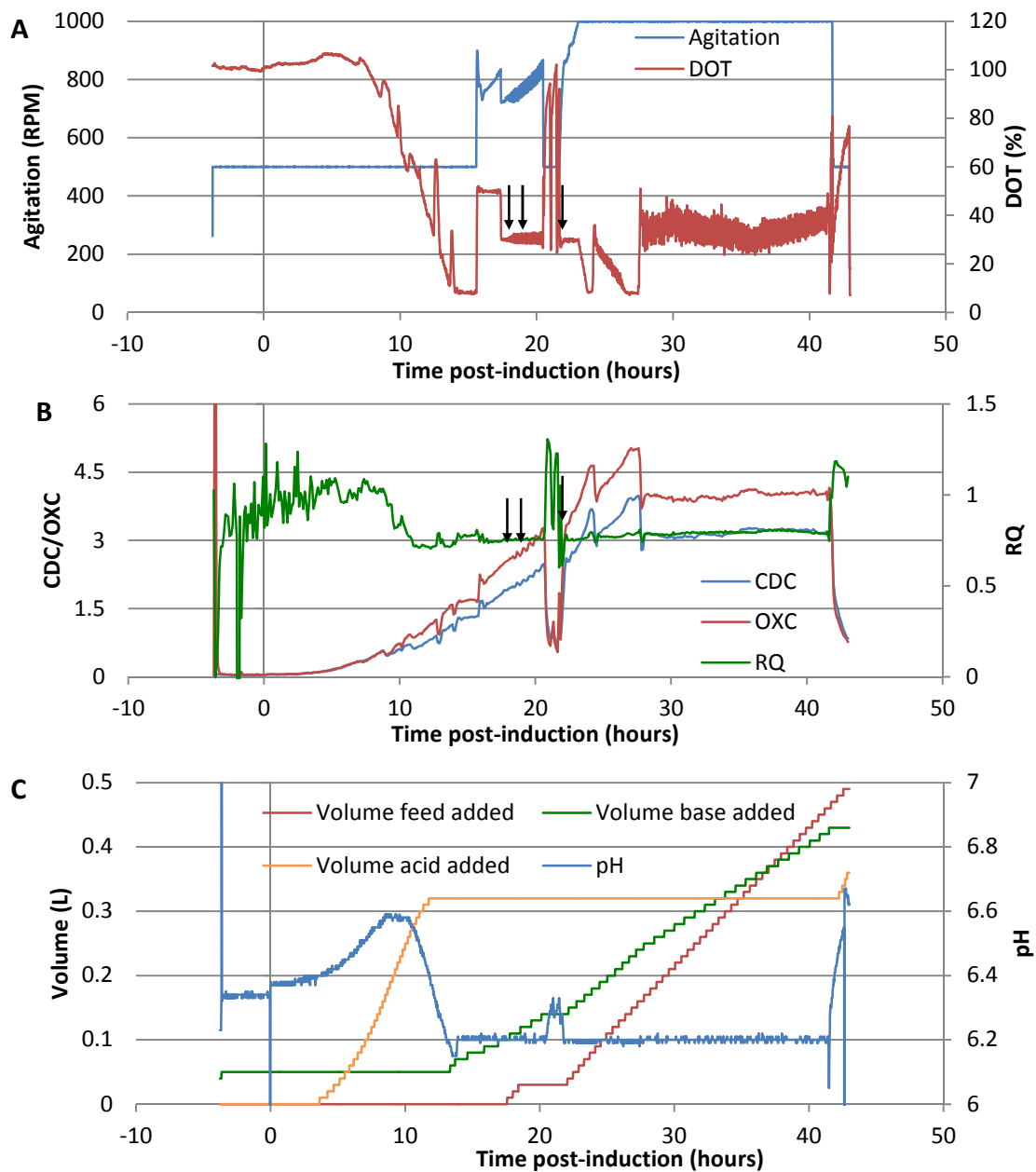
Supplemental figure 2. On-line data from a protocol B fermentation.

A - Agitation (red) and DOT (blue) data. B - Gas-MS data; CDC (blue) OXC (red), RQ (green). C - pH (blue), volumes of feed (red), acid (green) and base (orange) added to vessel.



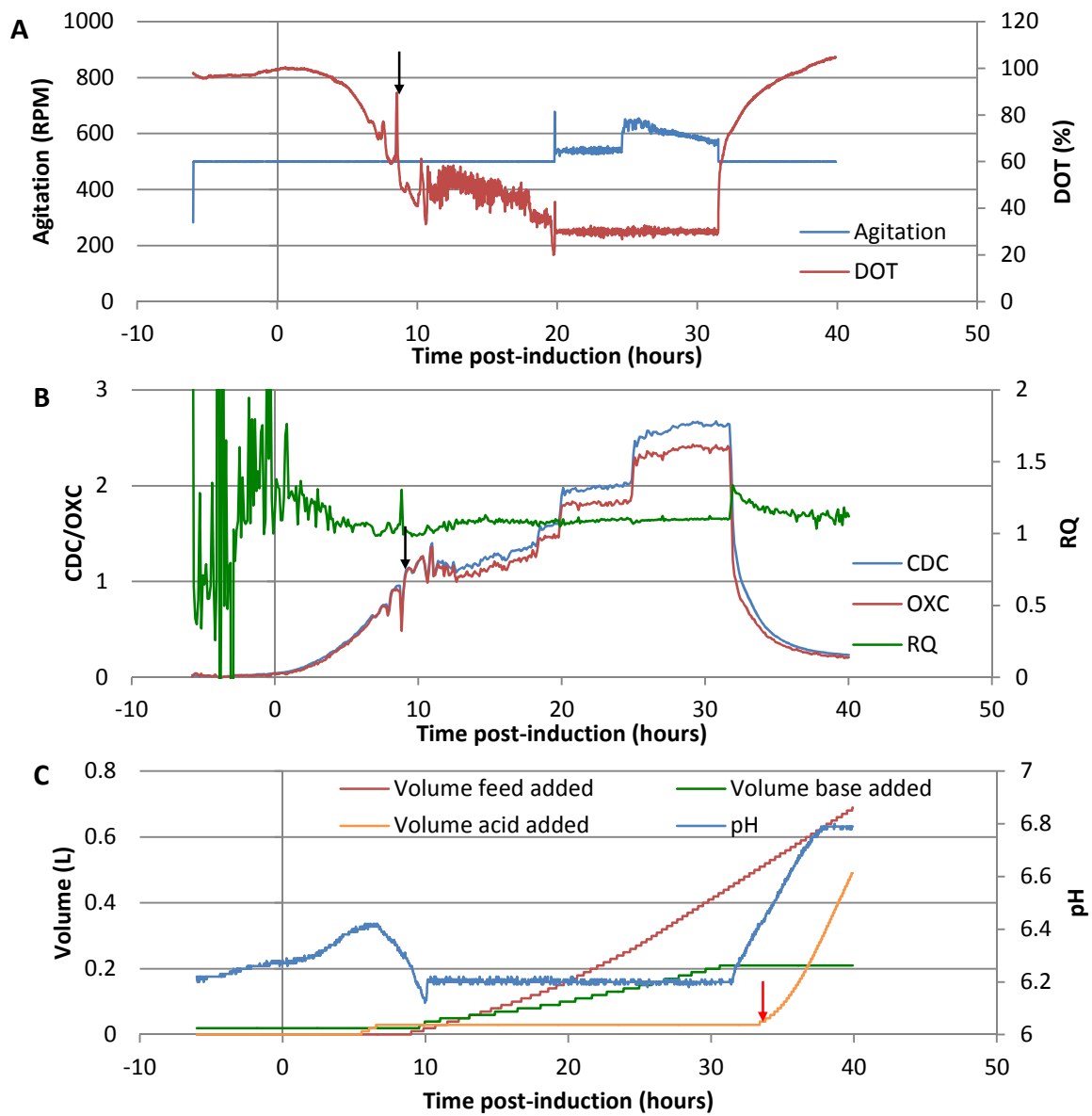
Supplemental figure 3. On-line data from a protocol C fermentation.

A - Agitation (blue) and DOT (red) data. B - Gas-MS data; CDC (blue) OXC (red), RQ (green). C - pH (blue), volumes of feed (red), base (green) and acid (orange) added to vessel. Data from a representative fermentation of a minimum of 2 replicates.



Supplemental figure 4. On-line data from a protocol D fermentation.

A - Agitation (blue) and DOT (red) data. B - Gas-MS data; CDC (blue) OXC (red), RQ (green). C - pH (blue), volumes of feed (red), acid (green) and base (orange) added to vessel. Data from a representative fermentation of a minimum of 2 replicates. Arrows indicate points at which feeding began or was paused (see text for details).



Supplemental figure 5. On-line data from a protocol E fermentation.

A - Agitation (blue) and DOT (red) data. B - Gas-MS data; CDC (blue) OXC (red), RQ (green). C - pH (blue), volumes of feed (red), base (green) and acid (orange) added to vessel. Black arrows indicate feeding, red arrow indicates point at which acid line became blocked and so after which no acid could be added to vessel. Acid addition trace is derived from fermenter software and reflects the revolutions of the acid addition pump. Data from a representative fermentation of a minimum of 2 replicates